AeroBest 2021
Lisboa, 21-23 July 2021

INVESTIGATING THE INFLUENCE OF UNCERTAINTY IN NOVEL AIRFRAME TECHNOLOGIES ON REALIZING ULTRA-HIGH ASPECT RATIO WINGS

Yiyuan Ma[1]*, Edmondo Minisci[2] and Ali Elham[1]

1: Institute of Aircraft Design and Lightweight Structures
Faculty of Mechanical Engineering
Technische Universität Braunschweig
35 Hermann-Blenk Street, 38108, Braunschweig, Germany
{Yiyuan.Ma, a.elham}@tu-braunschweig.de, https://www.tu-braunschweig.de/ifl

2: Intelligent Computational Engineering Laboratory
Faculty of Engineering
University of Strathclyde
75 Montrose Street, G1 1XJ, Glasgow, UK
edmondo.minisci@strath.ac.uk https://www.strath.ac.uk/staff/minisciedmondodr/

Abstract *This work studies the influence of uncertainty analysis on the unconventional aircraft conceptual design outcomes. The SBW and TF configurations are considered for the Short-Range (SR), Mid-Range (MR) and Long-Range (LR) missions, respectively. Conceptual design and analysis methodologies for the SBW and TF configurations are developed. Besides, the uncertainty analysis, constrained optimisation and global sensitivity analysis methodologies are presented. The proposed conceptual design methods are used to design an SBW and a TF aircraft for each mission, respectively, and the best-in-class configuration for each mission is initially obtained. Then the main uncertainties of each aircraft are identified and constrained optimisation is applied to find the best-case configuration with the objective function of the fuel weight. Moreover, a surrogate-based cut-HDMR method is used for the global sensitivity analysis to identify the most critical uncertainties and quantify their influences on the objective function. The results showed that according to the conceptual design results, the SBW configuration is the best-case for the SR mission, while the TF configuration is the best-case configuration for the MR and LR missions. Six main uncertainties, including four technologies-related and two mission-related parameters, are identified. The performed uncertainty analyses point out that, while there is not appreciable difference in terms of robustness against the operative and technology uncertainties for the SR mission configurations, the TF configuration is also more robust for MR and LR missions. Moreover, the sensitivity analyses assists in understanding which are the main uncertain drivers for each configuration and mission.*

Keywords: Uncertainty analysis, conceptual design, constrained optimisation, global sensitivity analysis, configuration comparative study

1. INTRODUCTION

Making future air transportation more sustainable and energy-efficient, the European Commission and NASA have put forward challenging goals for future-generation aircraft and funded numerous advanced technologies and projects to facilitate the early realization of these goals [1, 2]. The Ultra-High Aspect Ratio Wing (UHARW) configuration is one of the most promising approaches to improve aircraft fuel efficiency and reduce emissions.

For the UHARW concept application, some strategies need to be proposed to reduce the huge bending moment and shear force in the wing structure. Strut-Braced Wing (SBW) and Twin-Fuselage (TF) concepts are two promising aircraft configurations for the UHARW design, which could significantly reduce the wing bending moment through the strut support or the off-centreline located fuselages with their payloads. There have been many studies on the SBW configuration and the TF configuration. For example, the Subsonic Ultra Green Aircraft Research (SUGAR) project, carried out by NASA, Boeing and the Georgia Institute of Technology, has comprehensively researched the SBW configuration for the next-generation mid-range transport mission [1]. Hosseini et al. [3] investigated the application potential of the SBW concept in regional jet aircraft. Virginia Polytechnic and State University carried out the conceptual design and optimization of a long-range SBW passenger aircraft [4]. However, comprehensive research on the SBW configuration for different missions, including uncertainty analysis for the novel airframe technologies and operating parameters, is still lacking. Many different kinds of TF aircraft have been designed, developed and flight-tested, such as WhiteKnightTwo [5], a general aircraft HY4 [6] and a TF Unmanned Aerial Vehicle (UAV) [7] and so on. However, there is little published research on the TF passenger aircraft, which probably due to airport infrastructure constraints (e.g., runway width and terminal access).

Due to the scarcity of data during the conceptual design phase, expert knowledge elicitation can be used to quantify subjective judgements and use this information to properly characterize the uncertainties. Since during the conceptual design phase there are not enough elements to characterise the model uncertainties through “precise” probability functions the interval approach or the evidence theory can be used to model and propagate both aleatory and epistemic uncertainties expressed as a set of intervals or imprecise probability distributions. Based on the characterised uncertainties, the best and worst performance response as a function of the considered uncertainties, can be obtained through a minimization process (best) and a maximization optimization process (worst). Moreover, optimization under uncertainties can be performed, and best- and worst-case configurations can be obtained through a min-min optimization process (best case) and a min-max optimization process (worst case) on both design and uncertain parameters, as well as configurations giving the best trade-off in terms of belief, through a multi-objective optimization process.

Robust- and sustainable-by-design ultra-higH aspEct ratio wing and Airframe (RHEA) is a Europe Union-funded project within the Clean Sky 2 Joint Undertaking (https://www.rhea-cleansky2.org/). The RHEA research team, composed of TU Braunschweig (DE), University of Strathclyde (UK), Imperial College (UK), DNW Wind Tunnels (NL) and IRT-Saint Exupery (FR), aims to design future-generation passenger aircraft with ultra-high aspect ratio wings and associated airframe to improve aircraft fuel efficiency. To this end, the overarching objective of RHEA is to improve the aerostructural design and efficiency of UHARW by combining advanced numerical and experimental methods for Multidisciplinary Design and Optimisation (MDO). Eventually, Short-Range (SR), Medium-Range (MR) and Long-Range (LR) missions will be addressed by RHEA and a paradigm shift towards robust design methods will be introduced.

This paper combines aircraft conceptual design methodology and uncertainty analysis at the conceptual design phase to study the effect of novel airframe technologies on the aircraft conceptual design outcomes. The conceptual design methodology of unconventional aircraft configurations, including SBW and TF concepts, and the uncertainty parameter analysis methodology, are introduced. Six aircraft configurations are designed based on the unconventional aircraft conceptual design process, and uncertainty analysis and global sensitivity analysis are performed for each of the six aircraft. Finally, referring to the uncertainty analysis results, the best-case and worst-case configurations and the configuration giving the best trade-off in terms of belief are obtained for each mission.

2. METHODOLOGY

This section presents the unconventional aircraft conceptual design and analysis methodology used in this research which involves uncertainty analysis and sensitivity analysis.

2.1. Conceptual design methodology

2.1.1. Conceptual design and analysis environment

Since this project addresses the future-generation passenger aircraft, several novel airframe technologies, including Hybrid Laminar Flow Control (HLFC), advanced materials and structure concept and active load alleviation, are assumed to be available in the Entry Into Service (EIS) timeframe of the aircraft studied in this paper, i.e., 2040.

Natural Laminar Flow (NLF) can significantly reduce the viscous wing drag for subsonic aircraft [8]. However, mid-range and long-range passenger aircraft operating in the transonic region require high wing sweep angles to reduce wave drag, making it challenging to maintain a wide range of NLF on the wing. Therefore, the HLFC technology will be applied to RHEA aircraft. In recent years, composites have gradually replaced metallic material in aircraft structures. For the RHEA aircraft, advanced materials and structures, such as tow-steered composite material [9] and thin ply materials for Composite Fibre-Reinforced Polymers (CFRP) structures, will be considered with respect to the structural weight saving at the conceptual design stage. Besides, aircraft structures need to be sized according to the worst-case operating condition, which can be represented by load factors. If the maximum load factors can be reduced to +1.5g and -0.5g by using advanced active load alleviation technologies for future-generation passenger aircraft, the wing weight saving can even reach 45% [10]. However, an aircraft design considering these new technologies includes a considerable level of uncertainties. The influence of these uncertainties on the outcome of the aircraft design is addressed in this work and the uncertainty analysis method used in this paper is presented in the next section.

Since unconventional aircraft configurations, including SBW and TF, are studied in this work, the traditional aircraft conceptual design methodologies and tools need to be extended, making them feasible for unconventional aircraft concepts involved in this work. In this research, the open-source aircraft design environment Stanford University Aerospace Vehicle Environment (SUAVE) [11] is used for the multi-fidelity analysis of aircraft performance and missions. The conceptual design methods of SBW and TF configurations, especially weight estimation methods and the above-mentioned novel technologies' influences on the initial sizing, are developed and added to SUAVE, making SUAVE feasible for the unconventional aircraft configurations investigated in this project. An in-house initial aircraft sizing tool PyInit [12], which was developed by the authors, is used for the initial aircraft sizing and

preliminary performance analysis. Besides, OpenVSP is used for aircraft geometric modeling and visualisation.

2.1.2. SBW sizing methodology

In this module, the required thrust-to-weight/power-to-weight ratio and wing loading are first estimated, and then the components' initial sizing and preliminary aerodynamic analysis (a semi-empirical method) are carried out by using the modified PyInit. Then the initially sized aircraft is input into the SUAVE for the weight breakdown and missions iteration analysis.
As mentioned above, SUAVE needs to be extended for the SBW aircraft configuration in this study, especially the weight estimation module. A semi-empirical wing weight estimation method for SBW configuration developed by Chiozzotto [13] is used in this paper, which was developed from structural sizing analysis and could capture the influences of the strut reaction and the design features of the high aspect ratio wing. Besides, this wing weight estimation method also considers the aeroelastic phenomena. The total wing weight of SBW configuration, including wing and strut, is estimated by:

$$m_w = k_{\text{ail}} \left(m_{\text{covers}} + m_{\text{web+ribs}} \right) + m_{\text{sec}} + m_{\text{strut}} \tag{1}$$

where m_w is the total wing weight, k_{ail} is the weight penalty factor due to the aileron efficiency constraints, m_{covers} is the wing box covers mass, $m_{\text{web+ribs}}$ is the wing cox spar webs and ribs mass, m_{sec} is the wing secondary structure mass and m_{strut} is the strut mass. m_{covers} . $m_{\text{web+ribs}}$ and m_{strut} are estimated by using a regression formula. More detailed information on this wing weight estimation method can be found in Ref. [13]. In addition, it should be noted that this method has been validated by several conventional aircraft [13] and an SBW passenger aircraft [3].
Since the other components of the SBW aircraft, including fuselage, tails, engines, landing gears and so on, are similar to those of conventional aircraft, the Flight Optimization System (FLOPS) [14] is used for these components' mass estimation.

2.1.3. TF sizing methodology

Similar to the SBW sizing methodology, the required thrust-to-weight/power-to-weight ratio and wing loading are first estimated, and then the components' initial sizing and preliminary aerodynamic analysis are carried out by PyInit. It should be noted that the fuselage of the TF aircraft needs to be sized especially. In this paper, the fuselage sizing method presented by Torenbeek [15] is used, i.e., each fuselage's length and equivalent width equal to that of the reference fuselage multiplied by $\sqrt{2}$, which ensures the TF aircraft and the reference conventional aircraft have the same total cabin floor area, i.e., the same passenger capacity.
The weight estimation method for TF configuration is integrated into the SUAVE as well. A semi-analytical wing mass estimation method for TF aircraft developed by Udin [16] is used, which estimates the TF aircraft wing mass according to the wing spanwise load distribution, including aerodynamic load, fuel mass, wing structural mass and concentrated load. The TF aircraft wing structural mass is expressed as

$$m_{\text{s}} = k_{\text{sl}} k_{\text{tw}} k_{\text{man}} \left(m_M + m_Q \right) + m_{\text{rib}} + m_{\text{ail}} + m_{\text{sk}} + m_{\text{flap}} \tag{2}$$

where m_{rib}, m_{ail}, m_{sk} and m_{flap} are the secondary structure mass, k_{sl} is the service life factor, k_{tw} is the twist moment factor, k_{man} is the manufacturing factor and m_M and m_Q are the wing structural mass required to carry the bending moment and shear force, respectively, which are

shown in Figure 1. The detailed derivation process and integral calculations of this method can be referred to Ref. [16].

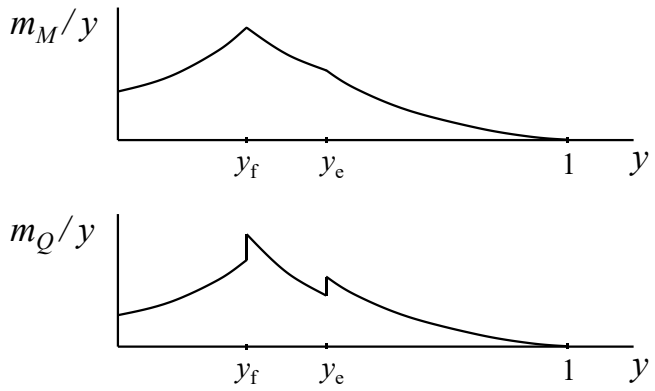

Figure 1. Spanwise distribution of relative wing mass [16].

Other components of TF aircraft, such as fuselage, tails, engines and so on, are similar to those of the conventional configuration, and the FLOPS method is used for these components' mass estimation.

2.2. Uncertainty analysis methodology

Six main uncertainties, four technologies related and two mission-related ones, have been identified. They include the achievable area of laminar flow over the wing, the achievable level of load reduction, the amount of structural weight reduction by using new materials and structures, the weight penalties on the wing due to folding mechanisms and the uncertainties on aircraft cruise Mach number and cruise altitude.
A file-based I/O process is implemented to interface the conceptual design tool with optimisers and sensitivity analysis codes and tools. The considered uncertainty inputs are:

- Cruise altitude, H_c
- Cruise Mach, M_c
- Vehicle range, R
- Maximum positive load factor, $n_{+,max}$
- Laminar transition (main wing), T_{Lw}
- Weight reduction factor (main wing), W_{Rw}
- Weight reduction factor (stabilizer), W_{Rs}
- Weight reduction factor (fuselage), W_{Rf}
- Wing weight penalty (due to the folding mechanisms), W_{Iw}

The conceptual design module has been interfaced with derivative-based and non-derivative-based search algorithms to explore the variability of the response W_f. The optimizer-conceptual design module coupling considers that the conceptual design module solves an internal constrained optimisation process to find the best sizing subject to a constraint on the payload weight, W_P.

- To estimate the variability of W_f due to the uncertainties, two optimisation processes have been performed for each tested configuration:
  - $\min_{\boldsymbol{U}} W_f$ (best case scenario)
- and
  - $\max_{\boldsymbol{U}} W_f$ (worst case scenario)

- where $\boldsymbol{U}=\{ H_c , M_c , R, n_{+,max} , T_{Lw} , W_{Rw} , W_{Rs} , W_{Rf} , W_{Iw}\}$.

To perform the sensitivity analysis and following ranking, the adaptive cut-High Dimensional Model Representation (A-cut-HDMR) [17,18,19] approach (a non-intrusive method similar to the Analysis Of Variance, ANOVA, decomposition) has been used. The A-cut-HDMR approach decomposes the general function response, $f(\boldsymbol{U})$, in a sum of the contributions given by each uncertainty variable and each one of their interactions through the model, considered as increments with the respect to the response in the anchor point (not necessarily the nominal response), f_c:

$$f\left(\boldsymbol{U}\right) = f_c + \sum_{i=1}^{n_u} F_i\left(U_i\right) + \sum_{i\le i<j\le n_u} F_{i,j}\left(U_i,U_j\right) + \ldots + F_{1,2,\ldots,n_u}\left(U_1,U_2,\ldots,U_{n_u}\right) \tag{3}$$

where n_u is the number of variables, and F_i, $i=1,\ldots,n_u$, are the orthogonal incremental contributions of every single uncertain parameter, $F_{i,j}$, $1 \le i < j \le n_u$, are the incremental contributions of each pair of uncertain parameters, and $F_{1,2,\ldots,n_u}$ is the incremental contribution of the interaction of all the uncertain parameters.

A surrogate model representation can be independently generated for each incremental contribution and only for the non-zero elements, thus greatly reducing the complexity of sampling and building the model. Moreover, the contribution of each term of the sum to the global response can be quantified independently so that higher-order interactions with low or zero contribution can be neglected already by analysing the lower-order terms.

This particular approach can be used to propagate any known standard distribution, from the classic Gaussian and uniform to Gumbell and Landau ones, and also non-standard distributions, as those deriving from the sum of kernels. The only assumption is the independence of the input uncertainties.

Not only is the output of this method the distribution of the quantity of interest, but also the quantification of the global contribution of each term of the sum to the global response. This feature allows for a complete analysis of the sensitivity of the response with respect to each of the stochastic variables, as well as their interactions. Moreover, in the case that the output function of interest is given by a black-box model, the analysis of the single contributions can give an insight into the structure of the response function.

The A-cut-HDMR is adaptive in terms of sampling and truncation of terms in Eq. (3). The adaptive sampling takes into account the shape of the underlying response and also the input probability distributions, leading to an efficient distribution of samples for the considered uncertainties and combination of uncertainties. The adaptive truncation removes the interactions that give a contribution to the overall response lower than a predefined threshold. The implemented heuristics for additivity have been demonstrated to be robust and efficient on a broad range of engineering cases.

2.3. Conceptual design and uncertainty analysis structure

The conceptual design and uncertainty analysis framework developed in this paper is shown in Figure 2. Firstly, PyInit is used to determine the constraint diagrams and size the aircraft dimensions, and then the initially sized aircraft and its operating conditions are input into the modified SUAVE for performance analysis. If the aircraft performance meets the design requirements, the initially designed aircraft will be transferred to the uncertainty analysis module. Otherwise, the design parameters will be adjusted in PyInit until the conceptual design process converges.

Constrained optimisation approaches are applied to find the best-case and worst-case configurations when the objective function is the fuel weight and the constraint on the

payload weight is implicitly imposed in the conceptual design module. Moreover, a surrogate-based cut-High Dimensional Model Representation (cut-HDMR) based approach, [19], is used to perform a global sensitivity analysis aimed at identifying the most critical uncertainties and quantifying their influence on the considered objective function.

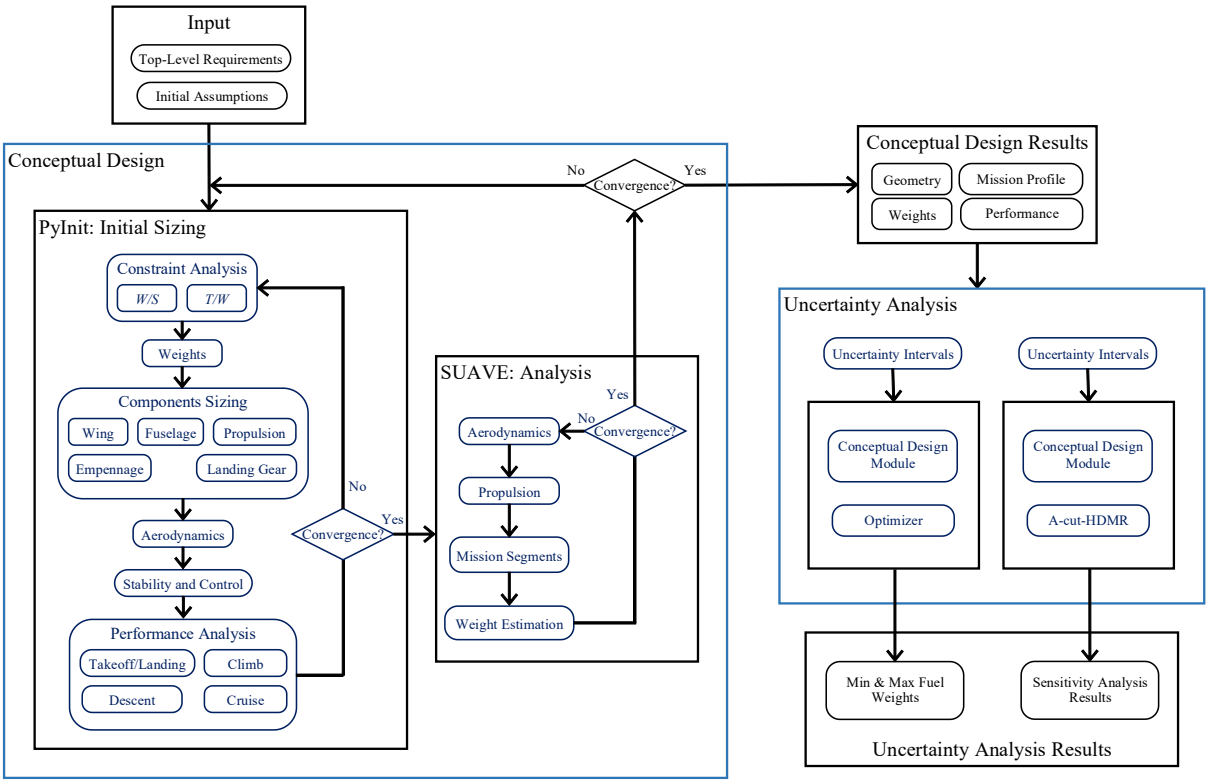

Figure 2. Conceptual design and uncertainty analysis structure.

3. AIRCRAFT CONCEPTUAL DESIGN AND UNCERTAINTY ANALYSIS

A total of six aircraft for the three missions are designed and studied in this section using the developed aircraft conceptual design and uncertainty analysis framework. According to the combination of aircraft performance analysis results and uncertainty analysis results, the best-case configuration of each mission is determined, and a comparison is conducted to study how the determination of the best-case and worst-case configurations is influenced by the uncertainty analysis. Besides, corresponding to the identified uncertainties, constrained optimisation is carried out to compare the SBW and TF aircraft for each mission. Then, the cut-HDMR method is used for the global sensitivity analysis of each aircraft to analyse the uncertainty characteristics.

3.1. Overview of the RHEA aircraft design requirements

The EIS of RHEA aircraft is taken as the year 2040, and RHEA aircraft is designed to comply with CS-25 certificate regulations [20]. The RHEA aircraft mission profile is shown in Figure 3. The entire mission is divided into several segments, including a main mission and a reserve phase. As the RHEA project aims at investigating the UHARW, the aircraft wing aspect ratio is initially taken as 25 in the conceptual design stage, which will be optimised in the later optimisation research phase. Besides, it should be noted that since the RHEA aircraft is designed with the UHARW concept, the wing may need to be designed to be foldable due to

airport facilities constraints.

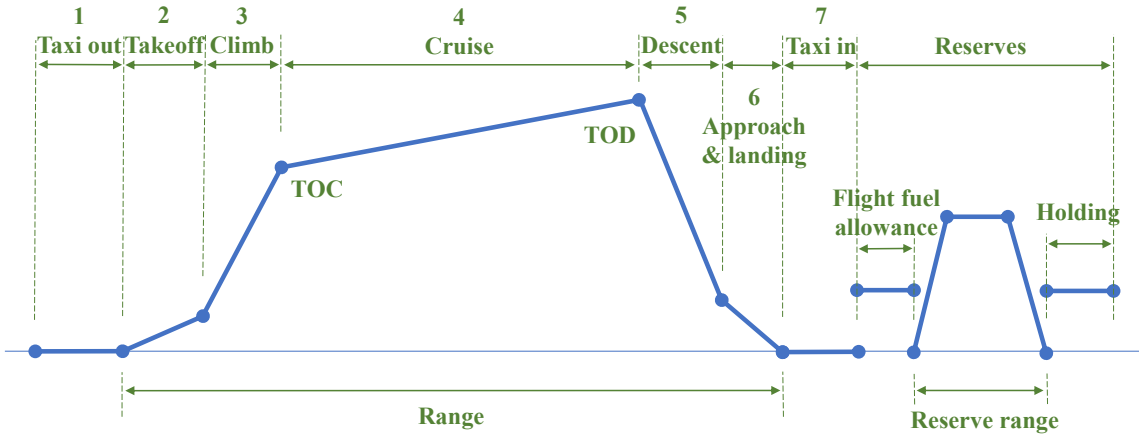

Figure 3. RHEA aircraft mission profile.

As described in Section 2.1, several novel airframe technologies for the next-generation passenger aircraft are considered in the RHEA aircraft design, including HLFC, load alleviation and advanced materials and structures. Assumptions for these novel technologies for different missions and different configurations are given in Table 1.

Table 1. Assumptions of novel airframe technologies.

Configuration		HLFC (Percentage of laminar flow area on the wing and tailplane)	Load alleviation (load factors)	Advanced materials & structures
Short-range	SBW TF	65% 70%	+1.5g and -0.5g	20% structural weight reduction
Mid-range	SBW TF	50% 55%	+1.5g and -0.5g	20% structural weight reduction
Long-range	SBW TF	50% 55%	+1.5g and -0.5g	20% structural weight reduction

3.2. RHEA aircraft conceptual design

According to the top-level aircraft requirements proposed in each subsection and the novel technologies assumed in Table 1, an SBW configuration and a TF configuration are initially sized by PyInit and analysed by SUAVE for each mission, respectively.

3.2.1. RHEA short-range aircraft

ATR 72-600 was selected as the reference aircraft for the SR mission. The top-level aircraft requirements of RHEA-SR aircraft are listed in Table 2. The RHEA-SR aircraft will operate at ICAO Class C airports, which requires that the aircraft wingspan should not exceed 36 meters and the main landing gear span should not exceed 9 meters (active constraint in the SR-TF aircraft configuration sizing).

Table 2. Top-level aircraft requirements of RHEA-SR aircraft.

Parameter	Unit	RHEA-SR

Reference aircraft		—	ATR 72-600
Propulsion concept		—	Turboprop
Cruise Mach number		—	0.42
Max. Mach number		—	0.457
Passengers		—	72
Range		nm	825
Reserves	Contingency fuel	—	3%
	Divert segment	nm	87
	Hold (at 1500 ft)	min	10
Cruise altitude		ft	20000
Service ceiling		ft	25000
Take-off field length		ft	4373
Landing distance		ft	3002
Approach speed		kt	113
Airport (ICAO C)	Wingspan	m	36
	Main landing gear span	m	9

The high-wing configuration with two turboprop engines was chosen for the RHEA-SR aircraft, and the wing was designed foldable with the folding position at 36 meters of the wingspan. NACA 65-618 and NACA 65-613 were chosen for the wing roots and wingtips to maximize the laminar flow range. The initially sized SR-SBW and SR-TF aircraft by PyInit are shown in Figure 4

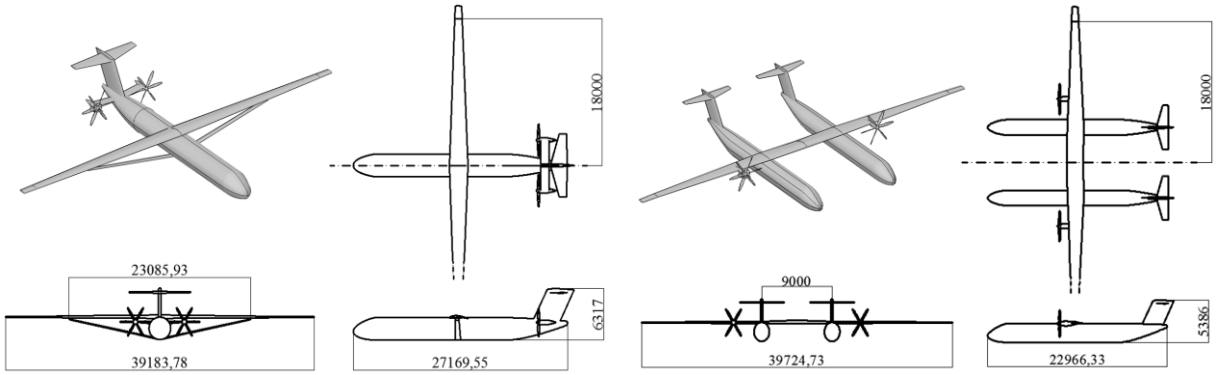

Figure 4. Three-view dimensions of RHEA-SR aircraft.

The fuselage of ATR 72-600 was used for the SR-SBW aircraft and was taken as the reference fuselage for the SR-TF aircraft, and both the SR-SBW and SR-TF aircraft were designed to have the same 72-seat capacity as the ATR 72-600. The SR-SBW aircraft uses the same fuselage interior arrangement as that of ATR 72-600, and the cabin interior arrangement of SR-TF aircraft is shown in Figure 5. It should be noted that the TF aircraft fuselage width was manually reduced to include a 2-abreast seating arrangement and the fuselage cross-section's height was slightly increased to the same height as the reference fuselage. In particular, two super-first-class seats are arranged at the non-cockpit fuselage nose with the best view, making full use of the fuselage space and providing more profits for airliners.

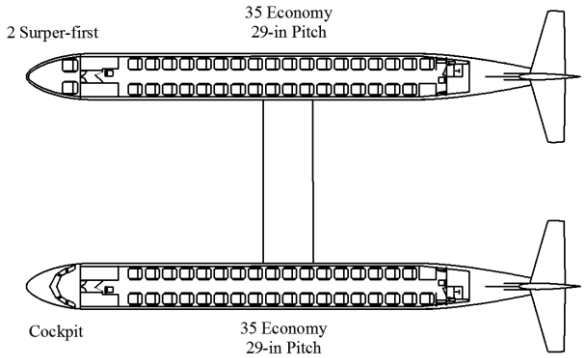

Figure 5. SR-TF aircraft interior arrangement.

Then the flight conditions and the initially sized SR-SBW and SR-TF aircraft were input into the modified SUAVE for performance analysis through iterative calculations. The SUAVE analysis results of the SR aircraft and the key weight data of the reference aircraft ATR 72-600 [21] are given in Table 3.

Table 3. Weight breakdown of short-range aircraft

Group	SR-SBW	SR-TF	ATR 72-600 [21]
MTOW, kg	22229	24028	22800
Fuel weight, kg	1432	2191	2000
Empty weight, kg	12821	13860	13500
Empty weight breakdown			
Wing, kg	2103	1556	
Fuselages, kg	2497	3052	
Propulsion, kg	1019	1094	
Nacelles, kg	269	287	
Landing gear, kg	643	690	
Horizontal tail, kg	201	414	
Vertical tail, kg	312	349	
Paint, kg	199	250	
Systems, kg	5579	6167	

Therefore, according to the aircraft dimensions in Figure 4 and the weight comparisons in Table 3, the SBW configuration outperforms the TF configuration in the SR mission because of its better fuel efficiency, lighter takeoff weight and smaller wingspan.

3.2.2. RHEA mid-range aircraft

A320neo was selected as the reference aircraft for the MR mission. The top-level aircraft requirements of RHEA-MR aircraft are listed in Table 4. The RHEA-MR aircraft will also operate at ICAO Class C airports.

Table 4. Top-level aircraft requirements of RHEA-MR aircraft.

Parameter	Unit	RHEA-MR
Reference aircraft	—	A320neo

Cruise Mach number		—	0.78
Max. Mach number		—	0.82
Passengers (1 class)		—	186
Passengers (2 class)		—	150
Range		nm	3400
Reserves	Contingency fuel	—	3%
	Divert segment	nm	200
	Hold (at 1500 ft)	min	10
Cruise altitude		ft	33000
Service ceiling		ft	38500
Takeoff field length		ft	＜6400
Landing distance		ft	＜4500
Approach speed		kt	136
Airport (ICAO C)	Wingspan	m	36
	Main landing gear span	m	9

Similar to the SR aircraft design, considering the UHARW concept, both the MR-SBW and MR-TF aircraft feature a high-wing configuration with two wing-mounted high bypass ratio turbofan engines, and the wings are designed to be foldable with the folding position at 36 meters of the wingspan. As the RHEA-MR aircraft will operate at the transonic region, the supercritical airfoils NASA SC(2)-0412 and NASA SC(2)-0410 were adopted for the wing root and wingtip airfoils, respectively, and NASA SC(2)-0010 was used for the tail airfoils. Besides, the wing sweep angle (0.25c) was taken as 12.5 deg to facilitate the laminar flow on the wing surface. OpenVSP was used for the aircraft visualization, and the initially sized MR-SBW and MR-TF aircraft are shown in Figure 6.

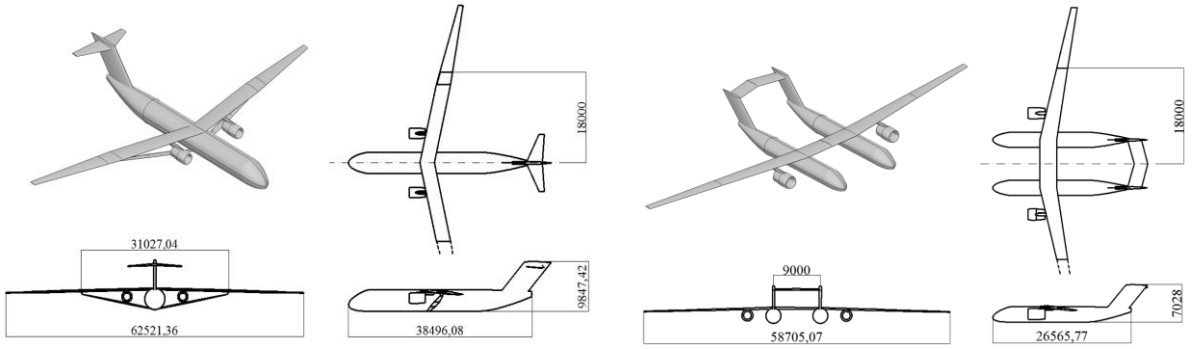

Figure 6. Three-view dimensions of RHEA-MR aircraft.

The fuselage of the A320neo was used for the MR-SBW aircraft and was taken as the reference for the MR-TF aircraft fuselage sizing, and both the MR-SBW and MR-TF aircraft were designed to have the same 150-seat arrangement as the A320neo. The MR-TF aircraft features a 4-abreast seating arrangement that meets the cabin parameter design requirements. In contrast, the reference A320neo has a 6-abreast seating arrangement in economy class. The cabin interior arrangement of the MR-TF aircraft is shown in Figure 7. Similar to the SR-TF aircraft design, two super-first-class seats are arranged in the non-cockpit fuselage nose.

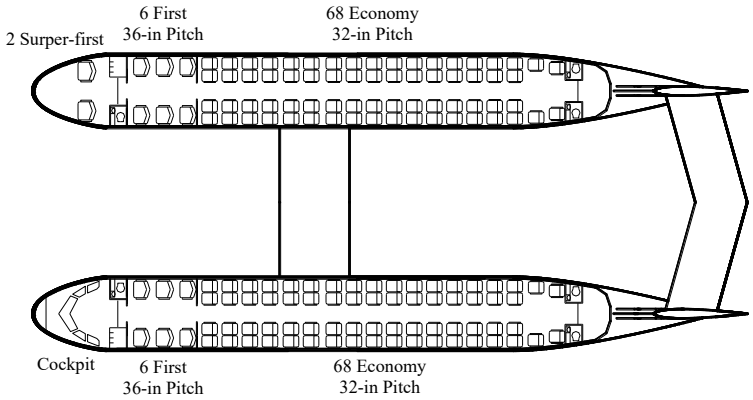

Figure 7. MR-TF aircraft interior arrangement.

Then the modified SUAVE was used to converge the aircraft weights while satisfying the required flight missions. The flight conditions and initially sized aircraft configurations of the MR-SBW and MR-TF aircraft obtained by PyInit were input into SUAVE for iterative calculations, respectively. The SUAVE analysis results of the MR aircraft and the key weight data of the reference aircraft A320neo [22] are listed in Table 5.

Table 5. Weight breakdown of mid-range aircraft

Group	MR-SBW	MR-TF	A320neo [22]
MTOW, kg	67929	57777	79000
Fuel weight, kg	16127	13328	20980
Empty weight, kg	37582	30229	44300
Empty weight breakdown			
Wing, kg	9393	4631	
Fuselages, kg	7066	5241	
Propulsion, kg	4493	3710	
Nacelles, kg	527	490	
Landing gear, kg	2292	1976	
Horizontal tail, kg	414	772	
Vertical tail, kg	902	844	
Paint, kg	447	415	
Systems, kg	12049	12151	

As given in Table 5, both SBW and TF configurations with the novel airframe technologies have significant advantages over the A320neo for the proposed mid-range mission. The MR-TF aircraft has significantly better fuel efficiency than that of MR-SBW aircraft, which is mainly due to the lighter operating empty weight. Besides, it is worth noting that the MR-TF aircraft's wing weight is significantly lighter than that of MR-SBW aircraft because of its better wing spanwise load distribution. Therefore, corresponding to the weight comparison in Table 5 and the aircraft dimensions in Figure 6, the TF configuration is the best-case configuration in the MR mission proposed in this paper.

3.2.3. RHEA long-range aircraft

B777-300ER was selected as the reference aircraft for the RHEA-LR mission. The top-level

aircraft requirements of RHEA-LR aircraft are listed in Table 6.

Table 6. Top-level aircraft requirements of RHEA-LR aircraft.

Parameter		Unit	RHEA-LR
Reference aircraft		—	B777-300ER
Cruise Mach number		—	0.84
Max. Mach number		—	0.89
Passengers (2 class)		—	350
Range		nm	7500
Reserves	Contingency fuel	3%	3%
	Divert segment	200	200
	Hold (at 1500 ft)	10	10
Cruise altitude		ft	35000
Service ceiling		ft	40000
Takeoff field length		ft	9000
Landing distance		ft	9000
Approach speed		kt	140
Airport (ICAO C)	Wingspan	m	65
	Main landing gear span	m	14

Due to the UHARW design, the high-wing configuration with two wing-mounted high bypass ratio turbofan engines was used for both the LR-SBW and LR-TF aircraft. The LR aircraft wings are designed to be foldable with the folding position at 65 meters of the wingspan. The supercritical airfoils NASA SC(2)-0412 and NASA SC(2)-0410 were adopted for the wing root and wingtip airfoils, respectively. A wing sweep angle (0.25c) of 23 deg was chosen as a trade-off between the wave drag and the laminar flow on the wing surface. OpenVSP was used for the aircraft visualisation, and the initially sized LR-SBW and LR-TF aircraft are shown in Figure 8.

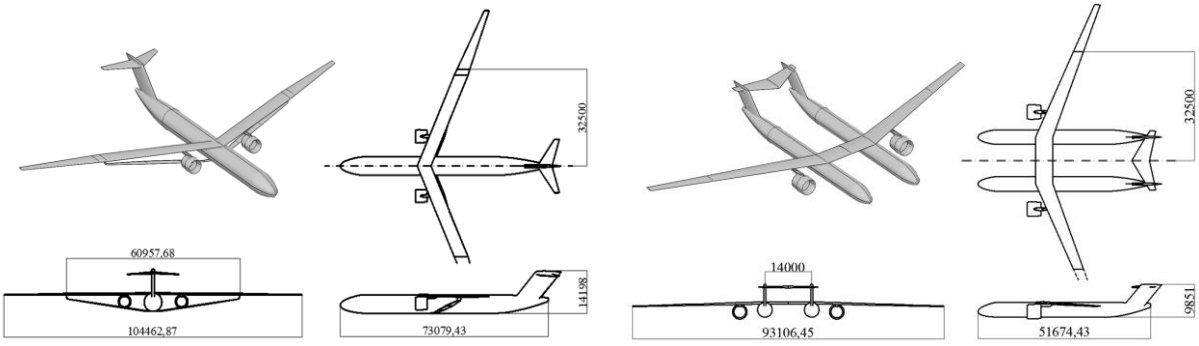

Figure 8. Three-view dimensions of RHEA-LR aircraft.

The fuselage of the reference aircraft B777-300ER was used for the LR-SBW aircraft and was taken as the reference for the LR-TF aircraft fuselage sizing. The LR-SBW and LR-TF aircraft were designed to have the same number of first- and economy-class seats. The reference aircraft B777-300ER and the LR-SBW aircraft feature a 6-abreast and 9-abreast

seating arrangement for the first-class and economy-class, respectively, while a 4-abreast first-class and 6-abreast economy-class seating arrangement was chosen for the sized LR-TF aircraft cabin, as shown in Figure 9. Besides, similar to the above-mentioned designs, the non-cockpit fuselage nose was arranged with two super-first-class seats.

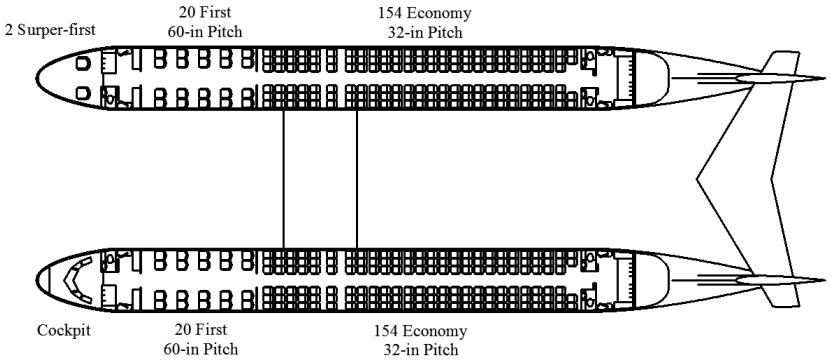

Figure 9. LR-TF aircraft interior arrangement.

The flight conditions and aircraft configurations of the LR-SBW and LR-TF aircraft obtained during the initial sizing by PyInit were input into the modified SUAVE for iterative calculations, respectively. The SUAVE analysis results of the LR aircraft and the key weight data of the reference aircraft B777-300ER [23] are tabulated in Table 7. Both SBW and TF configurations with the novel airframe technologies have significant advantages over the B777-300ER for the long-range mission. Due to the load distribution on the TF aircraft wings is more optimal than that of the SBW aircraft because the large centrally positioned fuselage weight is replaced by two outboard positioned weights, the TF aircraft wing weight is significantly lighter than that of the LR-SBW aircraft.

Table 7. Weight breakdown of long-range aircraft

Group	LR-SBW	LR-TF	B777-300ER [23]
MTOW, kg	262962	207105	351535
Fuel weight, kg	89716	79428	145538
Empty weight, kg	140066	94496	167829
Empty weight breakdown			
Wing, kg	47401	13687	
Fuselages, kg	25757	20596	
Propulsion, kg	18650	14774	
Nacelles, kg	2460	2255	
Landing gear, kg	7023	5639	
Horizontal tail, kg	1483	1515	
Vertical tail, kg	2923	2436	
Paint, kg	1237	1151	
Systems, kg	33133	32444	

As listed in Table 7, the LR-TF aircraft has a significantly better fuel efficiency than that of the LR-SBW aircraft. Therefore, the TF configuration is the best-case configuration in the LR mission due to its obvious performance advantages and its smaller size.

A summary of the RHEA aircraft conceptual design and initial comparison results are shown

in Figure 10, which will be further studied by uncertainty analysis in the next section.

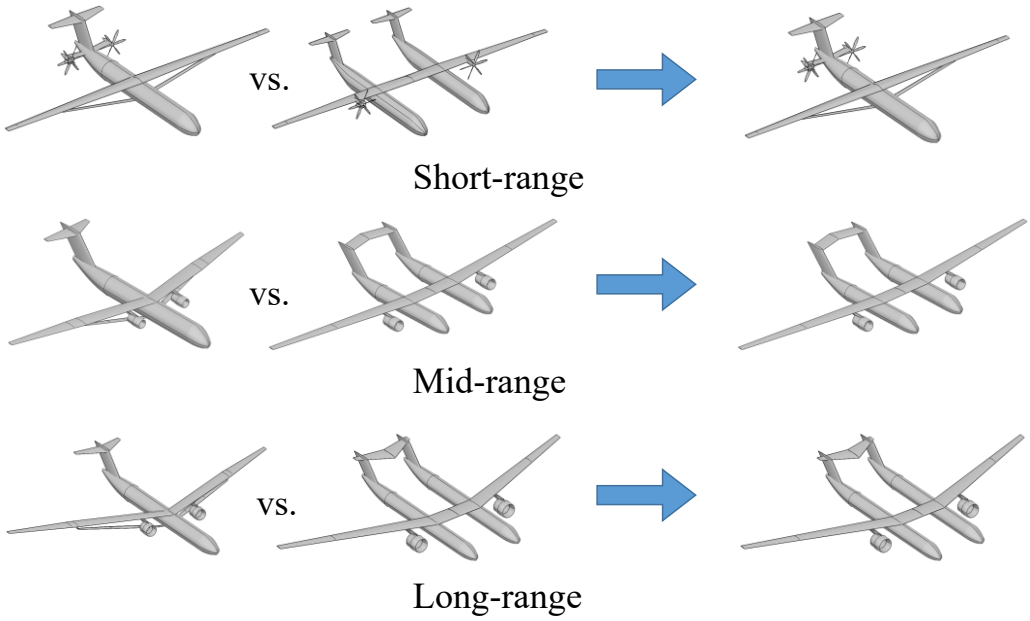

Figure 10. RHEA aircraft conceptual design results.

3.3. RHEA aircraft uncertainty analysis

Given the iterative process of the conceptual design module, the $W_f(\boldsymbol{U})$ function is very noisy, and to find the minima and maxima a combination of gradient-based and pattern search algorithms has been used. All the considered algorithms are part of the MATLAB optimization toolboxes.

3.3.1. Short-range configurations

For both cases (SBW and TF) the considered uncertainty bounds have been set as in Table 8 (***Lb*** and ***Ub*** values). The corresponding values for max and min of the performance function, W_f, are reported in the same table too.

The pursuit of the SBW best case scenario (minimisation process) brings to a sizing that allows $W_f = 1302\ kg$. The pursuit of the best-case scenario (maximisation process) brings to a sizing with $W_f = 1912\ kg$. The pursuit of the best-case scenario (minimisation process) brings to a sizing that allows $W_f = 2028\ kg$. The pursuit of the best-case scenario (maximisation process) brings to a sizing with $W_f = 2682\ kg$. It can be seen that from Table 8, for both configurations, the minimum value of W_f is obtained when the lower bound of H_c is considered, and, vice versa, then the maximum value is obtained when the upper bound of H_c is considered. The technology-related uncertainties play a role in accordance with a priori expectations. It is interesting to note that M_c does not play a role in this case, and this is also confirmed by the sensitivity analysis presented in Sec. 3.4.1

Table 8. Short-Rage: Lower and upper bounds (***Lb*** and ***Ub***, respectively) of the uncertain parameters, and values of uncertainty parameters giving the best case (min W_f) and the worst case (max W_f) sizings for the SBW and TF configurations.

ID	Uncertain parameters	*Lb*	*Ub*	Min W_f SBW	Max W_f SBW	Min W_f TF	Max W_f TF

1	H_c *[km]*	6.096	8.534	6.096	8.534	6.096	8.534
2	M_c	0.4	0.45	0.4	0.4	0.4	0.4
3	*R [nm]*	800	850	800	850	800	850
4	n_{+max} *[g]*	1.5	2.5	1.5	2.5	1.5	2.5
5	T_{Lw} *[%]*	0.5	0.5	0.75	0.5	0.75	0.5
6	W_{Rw} *[%]*	0.1	0.25	0.25	0.1	0.25	0.1
7	W_{Rs} *[%]*	0.1	0.25	0.25	0.1	0.25	0.1
8	W_{Rf} *[%]*	0.1	0.25	0.25	0.1	0.25	0.1
9	W_{Iw} *[%]*	0.05	0.1	0.05	0.1	0.05	0.1

3.3.2. Mid-range configurations

For both cases (SBW and TF) the considered uncertainty bounds and the corresponding values for max and min of the performance function, W_f, are reported in Table 9.
The pursuit of the SBW best case scenario (minimisation process) brings to a sizing that allows $W_f = 10617$ *kg*. The pursuit of the best-case scenario (maximisation process) brings to sizing with $W_f = 17872$ *kg*, which is very similar to the conservative nominal sizing.
The pursuit of the best-case scenario (minimisation process) brings to a sizing that allows $W_f = 9877$ *kg*. The pursuit of the best-case scenario (maximisation process) brings to a sizing with $W_f = 15229$ *kg*, which is again very similar to the conservative nominal sizing. It can be seen that in this case the H_c plays differently and the minimum value of W_f can be obtained for high cruise altitudes (vice versa for the maximum value). The cruise Mach now plays a more important role, and the achievable W_f increases in accordance with M_c.

Table 9. Mid-Rage: Lower and upper bounds (***Lb*** and ***Ub***, respectively) of the uncertain parameters, and values of uncertainty parameters giving the best case (min W_f) and the worst case (max W_f) sizings for the SBW and TF configurations.

ID	**Uncertain parameters**	***Lb***	***Ub***	**Min W_f SBW**	**Max W_f SBW**	**Min W_f TF**	**Max W_f TF**
1	H_c *[km]*	8.53	13.716	13.04	8.53	13.61	8.53
2	M_c	0.71	0.78	0.736	0.78	0.748	0.78
3	*R [nm]*	3300	3500	3457	3300	3300	3322
4	n_{+max} *[g]*	1.5	2.5	1.5	2.5	1.5	2.5
5	T_{Lw} *[%]*	0.5	0.75	0.75	0.5	0.75	0.5
6	W_{Rw} *[%]*	0.1	0.25	0.25	0.1	0.25	0.1
7	W_{Rs} *[%]*	0.1	0.25	0.25	0.1	0.25	0.1
8	W_{Rf} *[%]*	0.1	0.25	0.25	0.1	0.25	0.1
9	W_{Iw} *[%]*	0.05	0.1	0.1	0.1	0.1	0.1

3.3.3. Long-range configurations

For both cases (SBW and TF) the considered uncertainty bounds and the corresponding values for max and min of the performance function, W_f, are reported in Table 10.
The pursuit of the SBW best case scenario (minimisation process) brings to a sizing that allows $W_f = 58815$ *kg*. The pursuit of the best case scenario (maximisation process) brings to a sizing with $W_f = 121820$ *kg*. The pursuit of the best case scenario (minimisation process)

brings to a sizing that allows W_f = *56971 kg*. The pursuit of the best-case scenario (maximisation process) brings to a sizing with W_f = *94946 kg*. As for the short-range case, again W_f decreases with the cruise altitude and increases with the cruise Mach.

Table 10. Long-Rage: Lower and upper bounds (***Lb*** and ***Ub***, respectively) of the uncertain parameters, and values of uncertainty parameters giving the best case (min W_f) and the worst case (max W_f) sizings for the SBW and TF configurations.

ID	Uncertain parameters	*Lb*	*Ub*	Min W_f SBW	Max W_f SBW	Min W_f TF	Max W_f TF
1	H_c *[km]*	9.144	13.716	12.104	9.144	12.602	9.144
2	M_c	0.75	0.85	0.75313	0.813	0.76875	0.837
3	*R [nm]*	7400	7600	7600	7400	7600	7400
4	n_{+max} *[g]*	1.5	2.5	1.5	2.4375	1.5	2.5
5	T_{Lw} *[%]*	0.5	0.75	.75	0.5	0.75	0.5
6	W_{Rw} *[%]*	0.1	0.25	.2375	0.1	0.2375	0.1
7	W_{Rs} *[%]*	0.1	0.25	.25	0.1	0.175	0.1
8	W_{Rf} *[%]*	0.1	0.25	.2375	0.1	0.2375	0.1
9	W_{lw} *[%]*	0.05	0.10	0.05	0.1	0.075	0.1

3.4. Influence of uncertainties on the conceptual design outcomes

For this work, even if there are no data to properly characterise the distribution of input uncertainties, the A-cut-HDMR approach had been used considering uniform input distributions with the same bounds presented in tables included in Sec. 3.3 to perform the sensitivity analysis and rank the contributions of the single uncertainties as well as the possible contributions of the interactions. For each case, the tables in this section present the main contributions of the increment functions in absolute terms (6sigma, i.e. six times the standard deviation of each increment function) and relative terms (sensitivity variance, an index of relative ranking).

3.4.1. Sensitivity analysis for the short-range configurations

The adaptive sampling and related adaptive detection of important contributions bring to sensitivity analysis in terms of mean and variance sensitivity as shown in Table 11. The most important uncertainty contributions (measured as contribution to variance) for the SBW configuration, given the value of f_c = 1563 kg, are H_c (increment function 1) and T_{Lw} (increment function 5), followed by n_{+max}, (increment function 4) and M_c (increment function 2). The most important uncertainty contributions for the TF configuration, given the value of f_c = 2317 kg, are, again, H_c (increment function 1) and T_{Lw} (increment function 5), followed by M_c (increment function 2) and n_{+max}, (increment function 4).

Since short-range mission aircraft operate at low Mach numbers and aircraft performance is not very sensitive to compressive drag, the effect of cruise Mach number (i.e., *2* in Table 11) on both SR-SBW and SR-TF aircraft is minimal among the studied parameters. Mainly due to the high sensitivity of the turboprop engine performance to the operating altitude, this parameter has a significant impact on both SR-SBW and SR-TF aircraft. It is noteworthy that the cruise Mach number has the greatest effect on both configurations studied in this paper. Therefore, researchers should pay more attention to the cruise altitude when designing such aircraft. Besides, the laminar transition also plays an important role, which is consistent with a

previous preliminary estimation for an aircraft that features extended laminar flow along the airframes demonstrated a significant reduction (up to 50%) in overall drag [24]. And this impact on the TF configuration is significantly higher than that of the SBW configuration, which is due to the TF configuration has a shorter fuselage, so the TF configuration's tail area is larger than that of the SBW configuration. It is interesting to note that the maximum positive load factor $n_{+,max}$ has a more pronounced effect on the SBW configuration than the TF configuration, which may be due to the fact that the TF configuration has a better wing unloading effect than the SBW configuration, so that the $n_{+,max}$ has less effect on the TF configuration, and this phenomenon can also be observed in the MR and LR cases.

Table 11. Sensitivity analysis via A-cut-HDMR: main increment functions contributing to the variance of W_f for the SR-SBW configuration (left), and the SR-TF configuration (right)

Increment functions SBW	**Partial 6sigma for SWB [kg]**	**Sens. Variance SBW**		**Increment functions TF**	**Partial 6sigma for TF [kg]**	**Sens. Variance TF**
1	500	0.70229		*1*	444	0.4995
2	23	0.015		*2*	65	0.0105
4	145	0.0567		*4*	64	0.0103
5	287	0.2306		*5*	428	0.46325
8	35	0.0035		*8*	57	0.0082

3.4.2. Sensitivity analysis for the mid-range configurations

The adaptive sampling and related adaptive detection of important contributions bring to sensitivity analysis in terms of mean and variance sensitivity as shown in Table 12. The most important uncertainty contributions (measured as contribution to variance) for the SBW configuration, given the value of f_c = 12884 kg, are T_{Lw} (increment function 5) and H_c (increment function 1), followed by M_c (increment function 2) and n_{+max}, (increment function 4). The most important uncertainty contributions for the TF configuration, given the value of f_c = 11594 kg, are, again, T_{Lw} (increment function 5) and H_c (increment function 1), followed by M_c (increment function 2) and n_{+max}, (increment function 4).
Since the cruise phase of the MR mission accounts for a significant proportion in the whole mission, the laminar flow contributes the most to the aircraft performance due to the significant drag reduction. The most important contribution in the SR mission, i.e., the cruise altitude, also plays an important role in the MR mission, especially for the TF configuration. As explained in the sensitivity analysis for the SR mission (in Sec. 3.4.1), the contribution of the maximum positive load factor is more pronounced for the SBW configuration than for the TF configuration. As listed in Table 9, the Mach number's bounds considered for the MR mission were [0.71, 0.78], and the compressive drag in this range is not significant enough, so the sensitivity of the Mach number is relatively smaller than the others.

Table 12. Sensitivity analysis via A-cut-HDMR: main contributing increments functions for the MR-SBW configuration (left), and the MR-TF configuration (right)

Increment functions SBW	**Partial 6sigma for SWB [kg]**	**Sens. Variance SBW**		**Increment functions TF**	**Partial 6sigma for TF [kg]**	**Sens. Variance TF**
1	3145	0.24035		*1*	2917	0.35187

2	835	0.016947		*2*	813	0.027303
4	1886	0.086361		*4*	709	0.020773
5	5102	0.63224		*5*	3744	0.57959
1.2	739	0.013265		*1.2*	481	0.0095483

3.4.3. Sensitivity analysis for the Long-Range Configurations

The adaptive sampling and related adaptive detection of important contributions bring to sensitivity analysis in terms of mean and variance sensitivity as shown in Table 13. The most important uncertainty contributions (measured as contribution to variance) for the SBW configuration, given the value of f_c = 73021 kg, are n_{+max}, (increment function 4) and T_{Lw} (increment function 5), followed by M_c (increment function 2) and H_c (increment function 1). The most important uncertainty contributions for the TF configuration, given the value of f_c = 68033 kg, are, T_{Lw} (increment function 5) and M_c (increment function 2), followed by H_c (increment function 1), and, very marginally this time, by and n_{+max}, (increment function 4).
For the SR and MR missions, the distribution of the parameter sensitivity variances is essentially consistent with the two configurations. However, the sensitivity contributions of the parameters for the LR mission are significantly different between the SBW and TF configurations. According to the partial 6sigma values given in Table 13, it can be observed that this difference is mainly due to the different performance of the maximum positive load factor for these two configurations. As described in Sec. 3.4.1, because of the off-centreline located fuselages of the TF configuration, the wing unloading effect of this configuration is better than that of the SBW configuration, so the sensitivity contribution of the TF configuration's maximum positive load factor is smaller than that of the SBW configuration, and the difference in this contribution between these two configurations is greater than for the SR and MR missions since the off-centreline located fuselages are heavier in the LR mission, which is consistent with the weight breakdown data given in Table 7. Besides, similar to the MR mission, the laminar flow transition also has a significant impact on the SBW and TF configurations of the LR mission due to the large proportion of the cruise phase in the whole mission. The partial 6sigma results show that the cruise Mach's absolute influence value is similar for both configurations, while the cruise Mach's sensitivity variance of the TF configuration is much higher than for the SBW configuration due to the less contribution of the maximum positive load factor for the TF configuration. Finally, it should be noted that the cruise altitude is observed plays a more important role for the TF configuration than the SBW configuration.

Table 13. Sensitivity analysis via A-cut-HDMR: main contributing increments functions for the LR-SBW configuration (left), and the LR-TF configuration (right)

Increment functions SBW	**Partial 6sigma for SWB [kg]**	**Sens. Variance SBW**		**Increment functions TF**	**Partial 6sigma for TF [kg]**	**Sens. Variance TF**
1	6356	0.0183		*1*	13640	0.2064
2	13433	0.0818		*2*	14212	0.224
4	35971	0.5864		*4*	5867	0.0382
5	25988	0.3061		*5*	21457	0.5107
6	3081	0.0043		*6*	1682	0.0031
8	2578	0.003		*8*	2030	0.0046

				1.2	3406	0.0129

4. CONCLUSION

This paper addressed the influence of uncertainty analysis on the unconventional aircraft conceptual design outcomes. The SBW configuration and TF configuration were considered with respect to SR, MR and LR missions, respectively. Conceptual design and analysis methodologies for the SBW configuration and the TF configuration were first proposed. Six aircraft were preliminary designed by using the proposed methods and the best-in-class configuration of each mission was initially determined corresponding to the obtained performance analysis results. Then six main uncertainties, including four novel airframe technology parameters and two operating parameters, were identified and constrained optimisation approaches were applied to search for the best-in-class configuration. In addition, a surrogate-based cut-HDMR method was used to perform a global sensitivity analysis aimed at identifying the most critical uncertainties and quantifying their influences on the objective function. Finally, the best-case and worst-case configurations for each mission identified through uncertainty analysis and optimisation were compared with the initial conceptual design results, and the influence of uncertainties on the conceptual design outcomes was analysed.

Corresponding to the proposed top-level aircraft design requirements and novel technologies, an SBW configuration and a TF configuration aircraft were design for each mission, respectively, and their performance was analysed by using PyInit and SUAVE. The best-in-class configuration of each mission was obtained by comparing the fuel weight, takeoff weight and aircraft dimensions, i.e., the SBW configuration for the SR mission and the TF configuration for MR and LR missions.

The performed uncertainty analyses confirm the ranking of the different configurations and highlight which are the most critical aspects among the building technologies and the operative conditions that should be considered in the future design phases for each configuration, or at least for the configurations that will proceed further. In particular, the sensitivity analyses pointed out that: 1) while there is not appreciable difference in terms of robustness (measured here as difference between max and min W_f) against the operative and technology uncertainties for the SR mission configurations, the TF configuration is more robust for MR and LR missions; 2) the technology uncertainty that is always a major player, even if with different weights, for all the configurations is that related to the laminar to turbulence transition extension; 3) the operative conditions, i.e., cruise Mach and altitude, play a different role for each of the configurations and missions, and this should be taken into account for the next design phases.

ACKNOWLEDGMENTS

This project has received funding from the Clean Sky 2 Joint Undertaking (JU) under grant agreement No 883670. The JU receives support from the European Union's Horizon 2020 research and innovation programme and the Clean Sky 2 JU members other than the Union.

REFERENCES

[1] Greitzer, E. M., Bonnefoy, P. A., De la Rosa Blanco, E., Dorbian, C. S., Drela, M., Hall, D. K., ... and Mody, P., N+3 Aircraft Concept Designs and Trade Studies, Final Report. NASA/CR-2010-216794/VOL1, 2010.

[2] Anon., Realising Europe's Vision for Aviation: Strategic Research & Innovation Agenda, Vol. 1. Advisory Council for Aviation Research and Innovation in Europe, 2012.
[3] Hosseini, S., Ali Vaziri-Zanjani, M. and Reza Ovesy, H., Conceptual design and analysis of an affordable truss-braced wing regional jet aircraft. *Proceedings of the Institution of Mechanical Engineers, Part G: Journal of Aerospace Engineering*, 0954410020923060, 2020. doi: 10.1177/0954410020923060.
[4] Khan, K. H., Mallik, W., Kapania, R. K. and Schetz, J. A., Distributed Design Optimization of Large Aspect Ratio Wing Aircraft with Rapid Transonic Flutter Analysis in Linux. AIAA Paper 2021-1354, Jan. 2021. doi: 10.2514/6.2021-1354.
[5] Guerster, M. and Crawley, E. F. Dominant Suborbital Space Tourism Architectures, *Journal of Spacecraft and Rockets*, 56(5): 1580-1592, 2019. doi: 10.2514/1.A34385.
[6] Kallo, J., DLR Leads HY4 Project for Four-Seater Fuel Cell Aircraft. *Fuel Cells Bulletin*, 2015(11): 13, 2015. doi: 10.1016/S1464-2859(15)30362-X.
[7] Ma, Y., Zhang, W., Zhang, Y., Zhang, X. and Zhong, Y., Sizing Method and Sensitivity Analysis for Distributed Electric Propulsion Aircraft. *Journal of Aircraft*, 57(4): 730-741, 2020. doi: 10.2514/1.C035581.
[8] Beck, N., Landa, T., Seitz, A., Boermans, L., Liu, Y. and Radespiel, R., Drag Reduction by Laminar Flow Control. *Energies*, 11(1), 2018.
[9] Brooks, T. R., Martins, J. R. and Kennedy, G. J., High-Fidelity Aerostructural Optimisation of Tow-Steered Composite Wings. *Journal of Fluids and Structures*, 88: 122-147, 2019.
[10] Rossow, C., Geyr, H. and Hepperle, M., The 1g-Wing, Visionary Concept or Naive Solution? *DLR-IB-AS-BS-2016-121*, 2016.
[11] Lukaczyk, T. W., Wendorff, A. D., Colonno, M., Economon, T. D., Alonso, J. J., Orra, T. H. and Ilario, C., SUAVE: An Open-Source Environment for Multi-Fidelity Conceptual Vehicle Design. AIAA Paper 2015-3087, Jun. 2015.
[12] Karpuk, S. and Elham, A., Conceptual design trade study for an energy-efficient mid-range aircraft with novel technologies. *AIAA Scitech 2021 Forum*, January 2021. doi: 10.2514/6.2021-0013.
[13] P. Chiozzotto, G., Initial weight estimate of advanced transport aircraft concepts considering aeroelastic effects. AIAA Paper 2017-0009, Jan. 2015. doi: 10.2514/6.2017-0009.
[14] Wells, D. P., Horvath, B. L. and McCullers, L. A., The flight optimization system weights estimation method, NASA/TM-2017-219627/Volume I, 2017.
[15] Torenbeek, E., *Advanced aircraft design: conceptual design, analysis and optimization of subsonic civil airplanes*, John Wiley and Sons Ltd, West Sussex, 2013.
[16] Udin, S. V. and Anderson, W. J., Wing mass formula for twin fuselage aircraft, *Journal of Aircraft*. 29 (5): 907-914, 1992. doi: 10.2514/3.46261.
[17] Mehta, P.M., Kubicek, M., Minisci, E., Vasile, M., Sensitivity Analysis and Probabilisti c Re-entry Modeling for Debris using High Dimensional Model Representation based U ncertainty Treatment, *Advances in Space Research*, Vol.59, Issue 1, pp 193–211, Januar y 2017.
[18] Kubicek, M., High Dimensional Uncertainty Propagation for Hypersonic Flows and Ent ry Propagation, PhD Thesis, University of Strathclyde, 2018.
[19] Kubicek, M., Minisci, E. and Cisternino, M., High dimensional sensitivity analysis using surrogate modeling and High Dimensional Model Representation. *International Journal for Uncertainty Quantification*, 5(5): 393–414, 2015

[20] Certification Specifications and Acceptable Means of Compliance for Large Aeroplanes CS-25. June, 2020. URL https://www.easa.europa.eu/document-library/certification-specifications/cs-25-amendment-25.
[21] ATR-72 Series 600 Brochure. 2014. URL http://www.atraircraft.com/products_app/media/pdf/Brochure-ATR-600-Series_2014.pdf.
[22] Airbus S.A.S., A320 Aircraft Characteristics Airport and Maintenance Planning. Issue: 30 Sept. 1985, Rev: 1 April 2020.
[23] Airplanes, B. C. 2015. 777-200LR/-300ER/-freighter airplane characteristics for airport planning, Document Number D6-58329-2. URL http://www. boeing. com/assets/pdf/commercial/airports/acaps/777_2lr3er.pdf.
[24] Beck, N., Landa, T., Seitz, A., Boermans, L., Liu, Y. and Radespiel, R., Drag Reduction by Laminar Flow Control. *Energies*, 11(1), pp 252, 2018.